Intraductal xenografts show lobular carcinoma cells rely on their own extracellular matrix and LOXL1

APPENDIX.

Table of contents.

Appendix Figure Legend

Fig S1 Transcriptional profiling of ILC and Non-ILC ER+ HER2- patient tumor cells

A Table showing characteristics of primary breast tumors used in this study to generate intraductal PDXs.

B Experimental scheme showing the intraductal injection approach used to generate RNA sequencing data from ILC and non ILC ER+ HER2-PDXs. Breast cancer cells are transduced with RFP-luciferase expressing lentiviruses and injected via the teat into the milk ducts of NSG females. Tumor growth is monitored by bioluminescence imaging.

C Barplot showing the number of protein coding genes which are differentially expressed between ILC and non-ILC xenografts.

D Volcano plot showing differentially expressed genes between ILC and non-ILC patient derived tumor cells, n=3. All highlighted genes have *p*-values < 0.05 according to the limma model used for differential expression analysis. Genes with log2(FC) >0.5 in red and log2FC <0.5 in blue. Names of selected genes are indicated.

Fig S2 Bioinformatic analysis of genes differentially expressed between ILCs and non-ILC ER+ patient tumor cells

A-F RNA Sequencing was performed on ILC and non-ILC tumor cells derived by RFP-based FACS sorting from intraductal PDXs. Differentially expressed genes are ranked based on their p-value and fold change.

A-E GSEA plots showing correlation with genes differentially expressed in lobular carcinoma vs normal ductal breast cells (A), genes down-regulated in HMLE cells (immortalized nontransformed mammary epithelium) after *CDH1* knockdown by RNAi (B), genes involved in cell cycle (left), in G2M checkpoint (middle), and E2F target genes (right) (C), myc targets genes (left), mTOR (middle) and PI3K/AKT /mTOR signaling pathway genes (right) (D) as well as genes involved in interferon-alpha response (left), Androgen signaling response (middle), and TNFA Signaling via NFKB pathway (E).

F Motif activity response analysis associated with EPAS and BCL3 as well as FOXM1 and TBL1XR1 transcription factors as predicted by ISMARA.

Fig S3. TCGA breast tumors gene expression profiles of non-ILC and ILC.

A, B Violin plot showing normalized counts of ILC (n=127) versus non-ILC (n=490) of selected genes associated with matrisome (*ELN*, *COL1A1*, *COL6A1, COL14A1)*. Statistical significance determined by Student's unpaired t-test, two-tailed.

Fig S4. Global gene expression profle of SUM44 BAPN treated intraductal xenografts.

A, B Log10(radiance) curves of tumor growth for the MM134 (left) and SUM44 xenografts (right) treated early (A) and in the metastatic settings (B). For statistical analysis, mixed-effects linear models with spline regression (when applicable) were used. Likelihood-ratio tests were used for model comparison, i.e. to check whether the treatment/group covariate is significant.

C Principal component analysis (PCA) of RNAseq global gene expression data separating samples by treatment.

D Barplot showing the number of differential expressed protein-coding genes between vehicle and BAPN treated xenografts.

E Dotplot of log counts per million (CPM) from individual RNAseq samples (n=3) of selected genes.

F CNET plot of ReactomePA of genes up regulated in BAPN treated xenografts.

G Volcano plot showing genes, which are differentially expressed between vehicle and BAPN-treated SUM44 xenografts; N=3, all highlighted genes have p-values < 0.05 according to the limma model used for differential expression analysis. Genes with log2(FC) >0.5 in red and log2FC <0.5 in blue. Names of selected genes are indicated.

H GSEA plots showing gene sets that are differentially regulated between BAPN and PBS treated mice.

Fig S5. *LOXL1* knockdown and lLC growth.

A, B Log10(radiance) curves of tumor growth for the scramble and sh*LOXL1* MM134 (A) and SUM44 (B) xenografts. For statistical analysis, mixed-effects linear models were used. Likelihood-ratio tests were used for model comparison, i.e. to check whether the treatment/group covariate is significant

A

Tumor Number	Patient age (years)	% ER	% PR	Ki67 index	Subtype
69	75	100	100	16	ILC
73	69	100	0	26	ILC
76	31	100	60	80	non-ILC ER+ HER2-
78	78	100	80	10	ILC
81	39	98	10	35	non-ILC ER+ HER2-
99	57	100	70	20	non-ILC ER+ HER2-

B

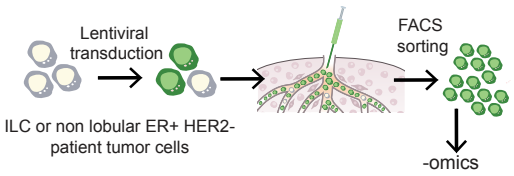

C

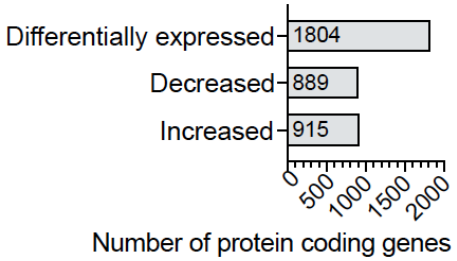

D

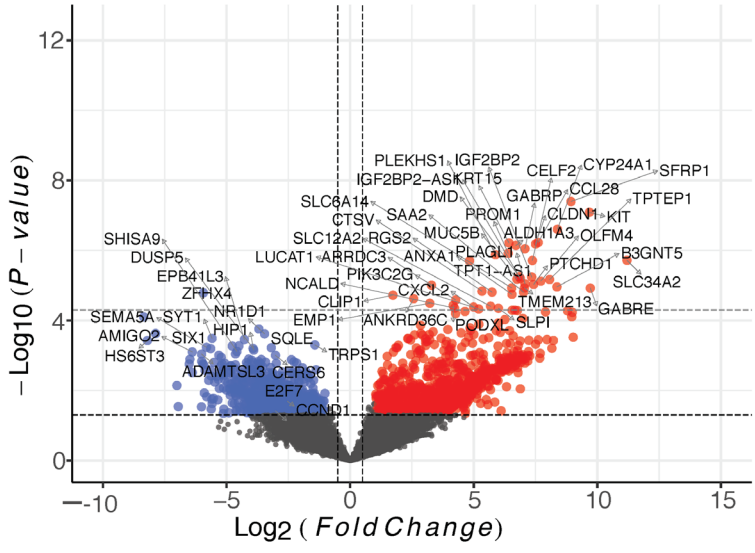

FC cutoff: 1; P−value cutoffs: 0.05, 5.0e-5

A

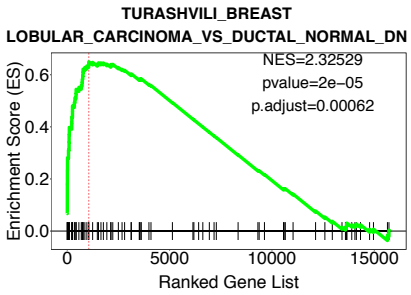
TURASHVILI_BREAST
LOBULAR_CARCINOMA_VS_DUCTAL_NORMAL_DN
NES=2.32529
pvalue=2e−05
p.adjust=0.00062
Enrichment Score (ES)
Ranked Gene List

B

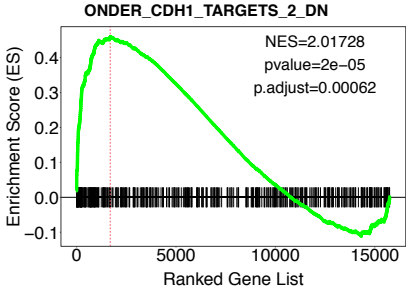
ONDER_CDH1_TARGETS_2_DN
NES=2.01728
pvalue=2e−05
p.adjust=0.00062
Enrichment Score (ES)
Ranked Gene List

C

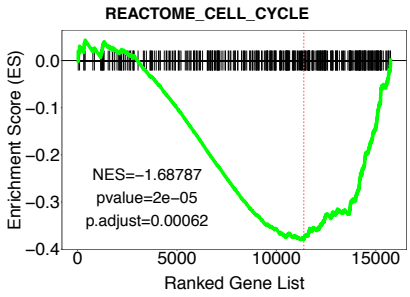
REACTOME_CELL_CYCLE
NES=−1.68787
pvalue=2e−05
p.adjust=0.00062
Enrichment Score (ES)
Ranked Gene List

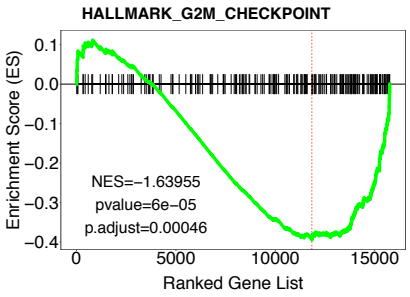
HALLMARK_G2M_CHECKPOINT
NES=−1.63955
pvalue=6e−05
p.adjust=0.00046
Enrichment Score (ES)
Ranked Gene List

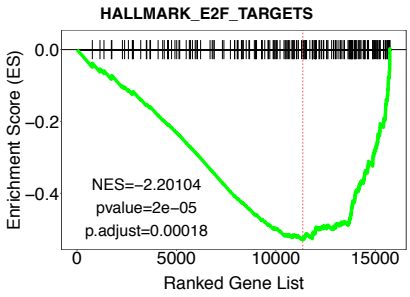
HALLMARK_E2F_TARGETS
NES=−2.20104
pvalue=2e−05
p.adjust=0.00018
Enrichment Score (ES)
Ranked Gene List

D

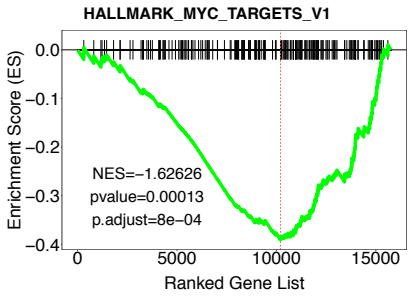
HALLMARK_MYC_TARGETS_V1
NES=−1.62626
pvalue=0.00013
p.adjust=8e−04
Enrichment Score (ES)
Ranked Gene List

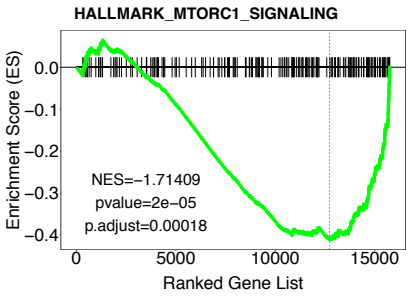
HALLMARK_MTORC1_SIGNALING
NES=−1.71409
pvalue=2e−05
p.adjust=0.00018
Enrichment Score (ES)
Ranked Gene List

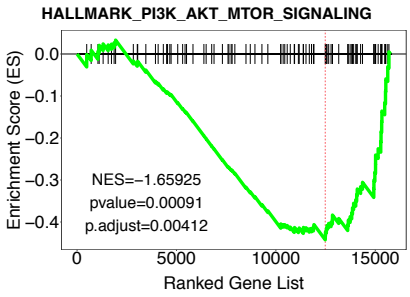
HALLMARK_PI3K_AKT_MTOR_SIGNALING
NES=−1.65925
pvalue=0.00091
p.adjust=0.00412
Enrichment Score (ES)
Ranked Gene List

E

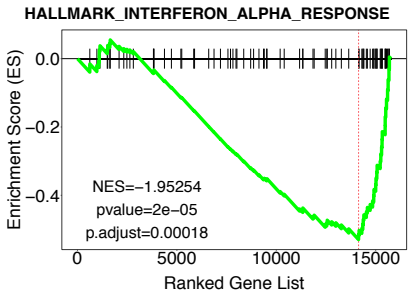
HALLMARK_INTERFERON_ALPHA_RESPONSE
NES=−1.95254
pvalue=2e−05
p.adjust=0.00018
Enrichment Score (ES)
Ranked Gene List

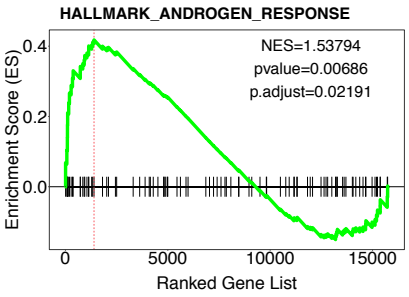
HALLMARK_ANDROGEN_RESPONSE
NES=1.53794
pvalue=0.00686
p.adjust=0.02191
Enrichment Score (ES)
Ranked Gene List

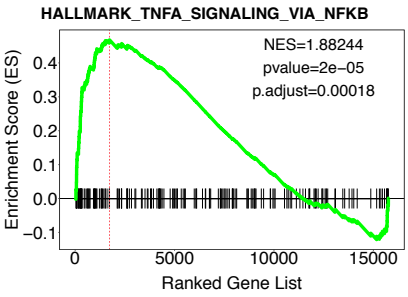
HALLMARK_TNFA_SIGNALING_VIA_NFKB
NES=1.88244
pvalue=2e−05
p.adjust=0.00018
Enrichment Score (ES)
Ranked Gene List

F

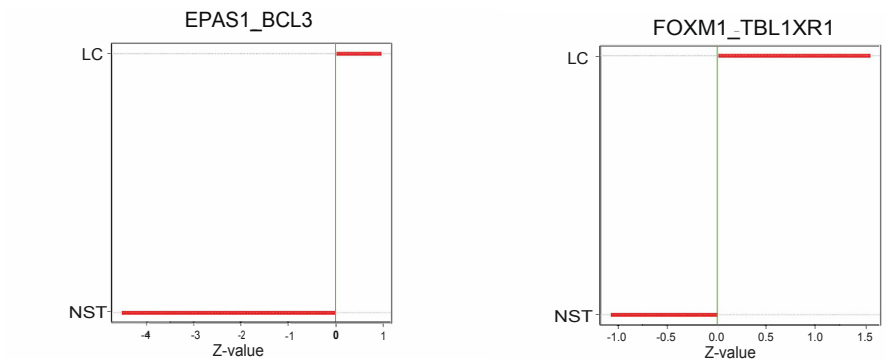
EPAS1_BCL3
LC
NST
Z-value
FOXM1_TBL1XR1
LC
NST
Z-value

Sflomos et al., Appendix Figure S3

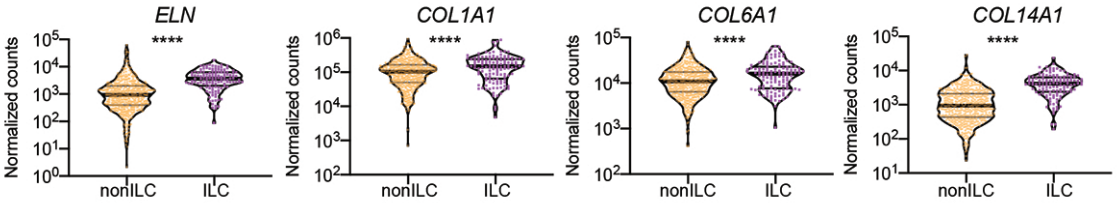

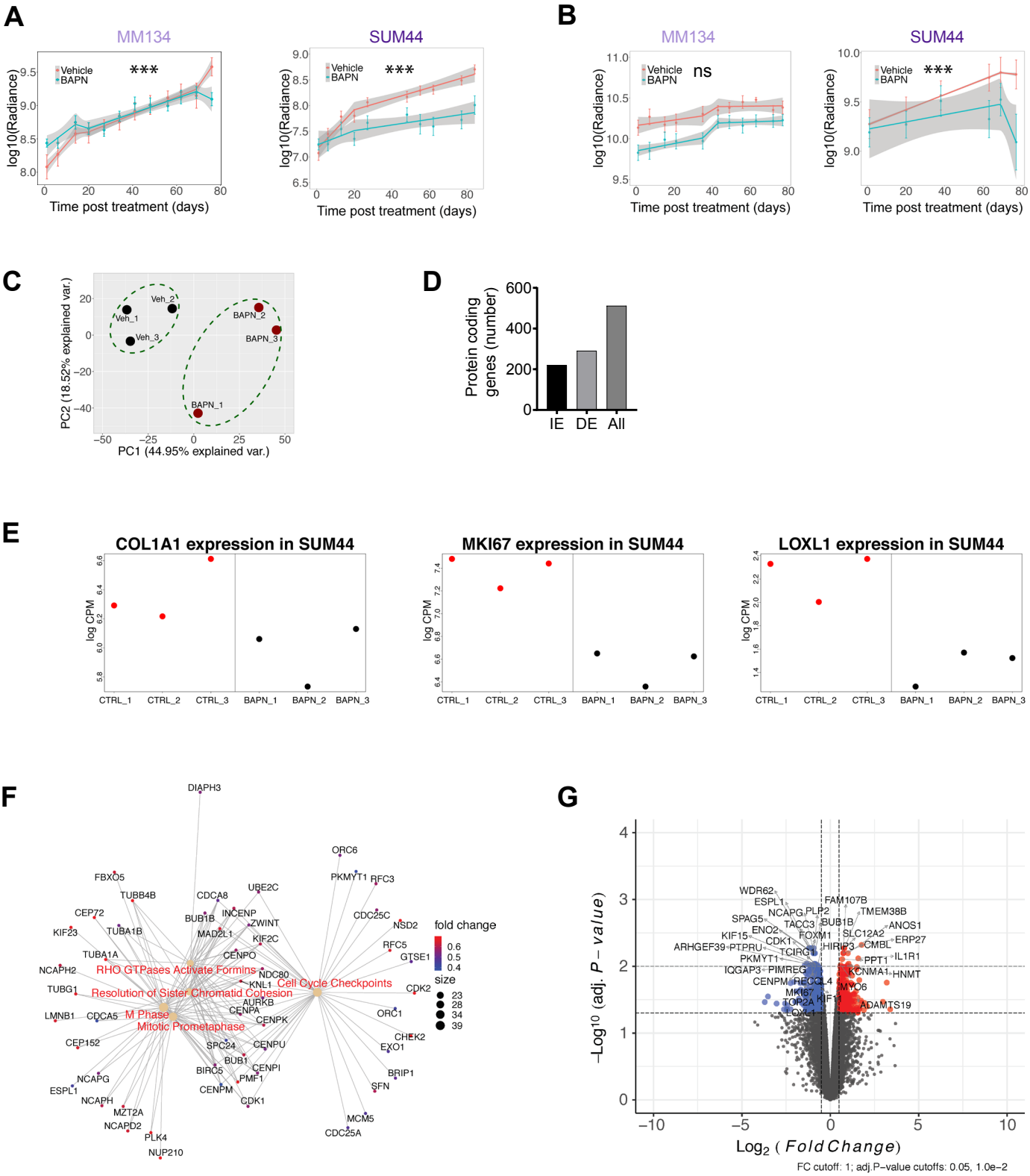
A
MM134
SUM44
Vehicle
BAPN
***
log10(Radiance)
Time post treatment (days)
B
MM134
SUM44
Vehicle
BAPN
ns
***
log10(Radiance)
Time post treatment (days)
C
PC2 (18.52% explained var.)
PC1 (44.95% explained var.)
Veh_1
Veh_2
Veh_3
BAPN_1
BAPN_2
BAPN_3
D
Protein coding genes (number)
IE
DE
All
E
COL1A1 expression in SUM44
MKI67 expression in SUM44
LOXL1 expression in SUM44
log CPM
CTRL_1
CTRL_2
CTRL_3
BAPN_1
BAPN_2
BAPN_3
F
DIAPH3
ORC6
FBXO5
PKMYT1
RFC3
TUBB4B
UBE2C
CDCA8
CEP72
BUB1B
INCENP
ZWINT
CDC25C
NSD2
KIF23
TUBA1B
MAD2L1
KIF2C
RFC5
GTSE1
TUBA1A
CENPO
NCAPH2
RHO GTPases Activate Formins
NDC80
KNL1
Cell Cycle Checkpoints
CDK2
TUBG1
Resolution of Sister Chromatid Cohesion
AURKB
LMNB1
CDCA5
M Phase
CENPA
CENPK
ORC1
Mitotic Prometaphase
CHEK2
CEP152
SPC24
CENPU
EXO1
BUB1
BIRC5
CENPI
BRIP1
NCAPG
PMF1
ESPL1
CENPM
SFN
NCAPH
CDK1
MZT2A
NCAPD2
MCM5
PLK4
CDC25A
NUP210
fold change
size
G
−Log10 (adj. P−value)
Log2 (FoldChange)
FC cutoff: 1; adj.P−value cutoffs: 0.05, 1.0e−2
H
HALLMARK_MITOTIC_SPINDLE
NES=−1.90704
pvalue=1e−05
p.adjust=0.00011
REACTOME_CELL_CYCLE
NES=−2.61775
pvalue=1e−05
p.adjust=3e−04
Enrichment Score (ES)
Ranked Gene List

Appendix Fig. S5

A

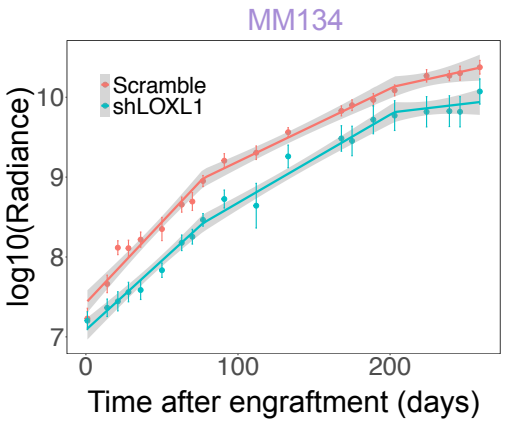

B

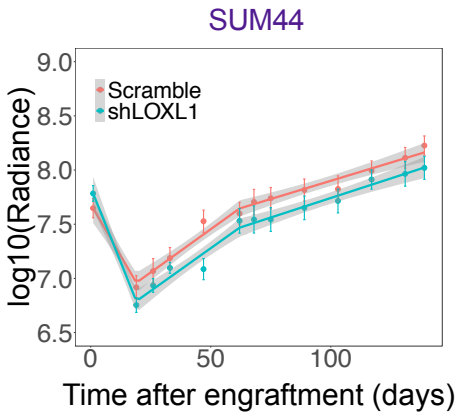

Appendix Table S1: Antibodies used in this study

Antibody - Target	Producer	Catalog Number	Species	Clone	Primary dilution	Used in Figures	*Gene*
Primaries							
LOXL1	Abcam	ab81488	Rabbit	na	1/200	Fig.4	*https://www.ncbi.nlm.nih.gov/gene/4016*
Ki67	Roche	790-4286	Rabbit	30-9	Ready to use	Fig.2	https://www.ncbi.nlm.nih.gov/gene/4288
ER	Roche	790-4286	Rabbit	SP1	Ready to use	Fig.2	https://www.ncbi.nlm.nih.gov/gene/2099
ER	Zytomed	RBK018	Rabbit	SP1	Ready to use	Fig.2	*https://www.ncbi.nlm.nih.gov/gene/2099*
ER	Santa Cruz	sc-8002	Mouse	F-10	1/200	Fig.4	*https://www.ncbi.nlm.nih.gov/gene/2099*
PR	Roche	790-2223	Rabbit	1E2	Ready to use	Fig.2	https://www.ncbi.nlm.nih.gov/gene/5241
E-cadherin	Cell signaling	sc-8426	Rabbit	G-10	1/400	Fig.2	*https://www.ncbi.nlm.nih.gov/gene/999*
SMA	Thermo Fisher Scientific	RB-9010	Rabbit	na	1/400	Fig.2J	https://www.ncbi.nlm.nih.gov/gene/59
GFP	Santa Cruz	sc-9996	Mouse	B-2	1/500	Fig.2I	*https://www.ncbi.nlm.nih.gov/protein/AAB51347.1?report=genbank&log$=protalign&blast_rank=1&RID=CB0V2C46015*
GFP	Thermo Fisher Scientific	PA5-22688	Rabbit	na	1/400	Fig.6	*https://www.ncbi.nlm.nih.gov/protein/AAB51347.1?report=genbank&log$=protalign&blast_rank=1&RID=CB0V2C46016*
Secondaries						Fig.2	
Alexa 568	Thermo Fisher Scientific	A-10042	rabbit	na	1/800	Fig.2	
Alexa 568	Thermo Fisher Scientific	A-10037	mouse	na	1/800	Fig.2	
Alexa 488	Thermo Fisher Scientific	A-21206	rabbit	na	1/800	Fig.2	
Alexa 488	Thermo Fisher Scientific	A-11029	mouse	na	1/800	Fig.2	

Appendix Table S2: Primers used in this study

Primer sequences		
Gene	**Forward (5' to 3')**	**Reverse (5' to 3')**
LOXL1	CTG TGC TGC GGA GGA GAA	GTA GTG GCT GAA CTC GTC CA
36B4	CTTCCCACTTGCTGAAAAGG	CGACTCCTCCGACTCTTCCT

Appendix Table S3: RNA scope probe for LOXL1 used in this study

Probe	**Cat. Number**	**Link**								
Probe- Hs-LOXL1	470751	https://acdbio.com/search/site/%252ALOXL1%252A/cms/probes/webspecies/human								

Author List 1 RLS: Gynecologists, oncologists, and pathologists who provided material support

Dr Didier JALLUT, General Director of RLS

Dr Pierre Bohanes

Dr Stéphane Cochet

Dr Marc Gander

Dr Aurélie Sivade

Dr Nam Tran

Dr Pierre-Michel GENOLET

Dr Nehad AKRAM

Dr Pierre KOVALIV

Dr Jean-Paul CHATELAIN

Dr Philippe BRACHER

Dr Catalin STAN

Dr Martine FRANCIOLI

Dr Catherine BECK

Dr Sylvia BONANOMI SCHUMACHER

Dr. Minh-Tri NGUYEN

Dr Ebtisam ALCHAB

Dr Bijan GHAVAMI

Dr Eric CHARDONNENS

Dr Frank GRUTTER

Dr Pu Yan

Dr Monika CHYZYNSKA

Dr Massimo Bongiovanni

Dr Lorenzo TAMINELLI